NADES-derived beta cyclodextrin-based polymers as sustainable precursors to produce sub-micrometric cross-linked mats and fibrous carbons

NADES-derived beta cyclodextrin-based polymers as sustainable precursors to produce sub-micrometric cross-linked mats and fibrous carbons

Claudio Cecone,[a] Gjylije Hoti,[a] Fabrizio Caldera,[a] Marco Zanetti,[a,b,c] Francesco Trotta,[a] and Pierangiola Bracco*[a]

[a.] Department of Chemistry, NIS Interdepartmental Centre, University of Turin, Via P. Giuria 7, Turin, 10125, Italy

[b.] Instm Reference Centre, University of Turin, Via G. Quarello 15A, Turin, 10135, Italy

[c.] ICxT Interdepartmental Centre, University of Turin, Via Lungo Dora Siena 100, Turin, 10153, Italy

Graphical abstract

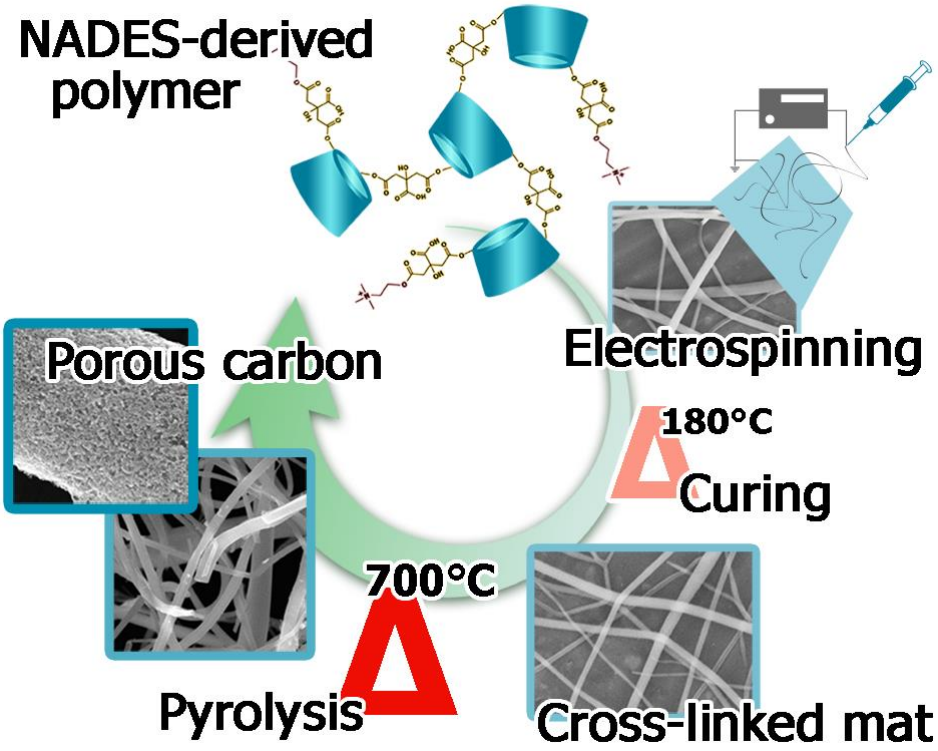

NADES-derived beta cyclodextrin-based polymers as sustainable precursors to produce sub-micrometric cross-linked mats and fibrous carbons

Claudio Cecone,[a] Gjylije Hoti,[a] Fabrizio Caldera,[a] Marco Zanetti,[a,b,c] Francesco Trotta,[a] and Pierangiola Bracco*[a]

[a.] Department of Chemistry, NIS Interdepartmental Centre, University of Turin, Via P. Giuria 7, Turin, 10125, Italy

[b.] Instm Reference Centre, University of Turin, Via G. Quarello 15A, Turin, 10135, Italy

[c.] ICxT Interdepartmental Centre, University of Turin, Via Lungo Dora Siena 100, Turin, 10153, Italy

Abstract

Owing to their tuneable synthesis, good chemical stability, and biocompatibility, beta cyclodextrin (βCD)-based polymers have attracted scientific and industrial attention. Besides, to render their fabrication more sustainable and suitable for large-scale productions, the substitution of toxic compounds and organic solvents with eco-friendly alternatives represents an active field of research. In this context, natural low-cost compounds such as sugars, carboxylic acids, and amino acids, have been extensively reported as suitable precursors to produce the so-called natural deep eutectic solvents (NADES). Furthermore, citric acid/choline chloride NADES systems have been exploited as suitable solvent/reactive media for the synthesis of functional water-soluble βCD-based polymers. In this work, the production of sub-micrometric fibres, from the electrospinning of NADES-derived βCD-based polymer solutions, was investigated, using water as a unique solvent. Also, the possibility to cross-link the obtained fibres via facile thermal treatment, without altering the fibrous morphology was demonstrated. Accordingly, cured, insoluble fibrous mats with mean diameters of 0.61±0.15 μm were obtained. Furthermore, the spun mats were screened as suitable bio-derived precursors to produce porous carbon fibres. Average diameters lower than 500 nm were obtained as a result, while the use of polyethylene oxide as a pore initiation agent, allowed to observe carbon fibres with porosities ranging from 13 to 24 nm. Eventually, the adsorption performances of both the cross-linked mat and the carbon fibres were tested for the treatment of emerging pollutants in contaminated water.

Keywords:

Cyclodextrins, natural deep eutectic solvents, bio-derived polymers, electrospinning, carbon fibres.

1. Introduction

The increasing demand for plastics observed during the past decades, and the subsequent waste accumulation, have emphasized the need to reduce the production of single-use plastic goods and to replace petrochemical-derived polymers with degradable choices, obtained through sustainable productions [1,2]. Furthermore, a

major industrial waste is represented by organic solvents, which raised significant concerns related to their disposal due to safety and pollution reasons [3–5]. As a consequence, the substitution of fossil-based products with eco-friendly choices has become an active field of research and one of the main aims of the Green Chemistry [6–8]. For this reason, environmental-friendly solvents and bioplastics are being studied and developed as sustainable replacements for a transition towards a circular economy [9]. In this regard, a sustainable alternative to organic solvents has recently been given by deep eutectic solvents (DES), liquid products obtained through the formation of an eutectic mixture of organic compounds, generally between two and three in number [10–15]. In addition, by exploiting natural low-cost products such as sugars, carboxylic acids, and amino acids, the so-called natural deep eutectic solvents (NADES) have been developed, where the use of choline chloride (CHO) and citric acid (CIT) -based systems has been extensively reported [16–18]. On the other hand, bioplastics are commonly defined as bio-based and/or biodegradable polymers, which can be broadly divided into (i) polymers that are both bio-based and biodegradable, (ii) polymers that are only bio-based, (iii) and polymers that are only biodegradable [19]. The first group comprises polysaccharides such as starch and cellulose but also lignocellulosic fibres, materials that attracted a great scientific and industrial interest mostly associated with their intrinsic safety [20–26]. Therefore, they have been exploited for packaging, food, environmental, pharmaceutical, and medical applications [27–35].

In this frame, starch enzymatic conversion products, beta cyclodextrins (βCDs) are cyclic truncated-cone-shaped molecules composed of seven α-(1,4)-linked glucopyranose units surrounding a slightly lipophilic inner cavity [36,37]. The presence of this peculiar domain enables the latter to accommodate guest molecules through the formation of inclusion complexes [38–41]. In addition, the hydroxyl functionalities owned by βCD, make them suitable building blocks for the synthesis of different polymer structures [42–44]. Both water-insoluble (cross-linked) and water-soluble (linear or hyper-branched) polymers have been developed by exploiting proper synthetic conditions and suitable cross-linkers, such as organic carbonates, dianhydrides, poly-carboxylic acids, diisocyanates, and diglycidyl ethers [45–47]. Besides, owing to their tuneable synthesis, good chemical stability, and biocompatibility, βCD-based polymers have been widely applied as drug carriers, gas traps, fillers, photo-stabilizers, adsorbents, and fire-retardant agents [48–54]. However, the use of organic solvents or toxic reactants has been often reported as a synthetic approach. For this reason, achieving the same goal with green alternatives would lead to more sustainable and eco-friendly processes suitable for large-scale productions, improving this class of materials [55–59]. The use of βCD in combination with NADES systems has been already reported for extracting, encapsulating, and catalytic scopes, while the synthesis of βCD-based polymers has been recently reported by our group, using CHO/CIT-based NADES as solvent/reactive media [60–69]. The peculiarity of this functional water-soluble product is that it can be turned into a cross-linked, water-insoluble product, via facile thermal treatment. This feature allows the processing of the aforementioned polymer into specific morphologies e.g., fibres or particles, starting from its water solutions, before securing the chosen form via cross-linking, for further applications.

In this context, electrospinning is a facile, cost-effective, and flexible approach that allows the production of fibres at micron, submicron and nano-scale, from an electrically charged jet of polymer solutions or melts [70].

Starting from the last decades, the development of this technique has now consolidated its role in the processing of a rich variety of polymers mostly for filtration, biosensors, drug delivery, tissue engineering, and wound dressings applications [71–74]. However, organic solvents are often required to obtain polymer solutions and this represents a limitation for many industrial productions due to environmental and safety regulations [75–78]. With the above in mind, the possibility to obtain fibrous mats via electrospinning from NADES-derived βCD-based polymer would allow to obtain a novel fibrous system, avoiding the use of any organic solvent, fossil-derived polymer, or toxic compound, describing a sustainable process.

Furthermore, bio-derived products such as wood, nutshells, and starch, have been also studied as a precursor for the production of activated carbons, materials characterised by a porous structure with surface area ranging from 500 to more than 2000 m^2/g [79–83]. Thanks to this feature, they display good adsorption capability towards a wide variety of organic and inorganic pollutants, while the choice of the precursor represents a key factor to obtain a good surface development and good structural characteristics [84–86].

Besides, the development of high-performance energy storage systems, observed as a consequence of the widespread application of electric devices and vehicles, has required power sources with high power densities, long cyclic life, and enhanced safety [87,88]. In particular, great interest has been given to rechargeable lithium-based batteries and supercapacitors, where carbon materials have been widely employed in the electrodes, as conductive additives, and as substrates for supporting metal oxides, due to their electrical conductivities, surface areas, and chemical stability [89]. In this frame, carbon nanofibers displayed several advantages, if compared to other carbon materials, thanks to the high aspect ratio which enables the formation of a conductive network [90,91].

Approximately 90% of the commercial carbon fibres are produced from polyacrylonitrile-based systems or mesophase pitch, and due to their excellent mechanical properties and thermal stability, they have been extensively applied to reinforce polymer-based composites for aerospace, automobile, sporting applications, and construction industries [91–94]. However, the petrochemical nature of the precursors and the costs associated with the production process, represent a limit on the availability of these goods.

In the awareness that both granular and fibrous βCD-based polymers have been reported to be effective microporous carbons precursors [95–97], in this work, a water-soluble βCD-based polymer, synthesized using a functional CHO/CIT-based NADES, was studied to produce novel environmentally-friendly bio-based fibres. These fibres were obtained via electrospinning technique utilizing sustainable processing conditions. Furthermore, the possibility to turn the so-obtained water-soluble polymer fibres into water-insoluble ones without altering the morphology, via facile thermal treatment, was evaluated. Eventually, the pyrolysis of the spun substrates was screened as an approach to produce fibrous carbons, while the pyrolysis of fibres obtained from blends of βCD-based polymer and polyethylene oxide, added as a pore initiation agent, was evaluated to modulate the porosities of the resulting carbon fibres.

2. Experimental

2.1 Materials

βCD were provided by Roquette Freres (Lestrem, France), while citric acid (CIT), choline chloride (CHO), sodium hypophosphite monohydrate (SHP) polyethylene oxide (PEO, Mw 600,000 Da), sodium hydroxide (NaOH), hydrochloric acid (HCl), oxalic acid, orthophosphoric acid, acetonitrile, and atenolol were purchased from Sigma-Aldrich (Darmstadt, Germany). βCD and CHO were dried in an oven at 75°C up to constant weight before use.

2.2 Polymer synthesis

The synthesis of the polymer was carried out with a procedure previously developed by our research group [69]. Firstly, the NADES was prepared by mixing in a round-bottom flask, 2.66 g of dry CHO and 7.34 g of dry CIT. The physical mixture was heated up at 140°C until a clear and transparent liquid was observed. Afterwards, by keeping the NADES at 140°C, 1.00 g of βCD and 0.10 g of SHP, as a catalyst, were added. A transparent liquid was obtained after 20 to 30 seconds of stirring under a vacuum using a diaphragm pump. Subsequently, the flask was cooled down to 110°C, at atmospheric pressure. The reaction was then carried out at 110°C under a vacuum for 6 hours. At the end of the reaction, the product appeared as a yellow to light brown bulk solid. The polymer was further recovered from the round-bottom flask by crushing it with a spatula. Then it was solubilized in distilled water at room temperature and purified by ultrafiltration (cut off 10 kDa) to separate the actual polymer from non-reacted βCD, reactants, and oligomers. The polymer solution was then recovered from the ultrafiltration cell and subsequently freeze-dried, obtaining a pale-yellow powder. The average molecular weight of the resulting polymer was 19 kDa [69].

2.3 Characterisation

Thermogravimetric analyses (TGA) were carried out using a TA Instruments Q500 TGA (New Castle, DE, USA), from 50°C to 700°C, under nitrogen flow, with a heating rate of 10°C/min.

A Perkin Elmer Spectrum 100 FT-IR Spectrometer (Waltham, MA, USA) equipped with a Universal ATR Sampling Accessory was used for FTIR-ATR (Attenuated Total Reflection) characterisation. All spectra were collected in the wavenumber range of 650-4000 cm^{-1}, at room temperature, with a resolution of 4 cm^{-1} and 8 scans/spectrum.

The chemical composition of the samples was studied using a Thermo Fisher FlashEA 1112 Series elemental analyser (Waltham, MA, USA).

A Malvern Zetasizer Nano-ZS (Malvern, United Kingdom) was used to measure the zeta (ζ)-potential. All the tests were performed using distilled water at room temperature.

The morphology of the samples was studied using scanning electron microscopy (SEM). The images were acquired with a Tescan VEGA 3 (Brno, Czech Republic) using secondary electrons and 15 kV accelerating voltage. Prior to SEM characterisation, the samples were ion-coated with gold using a Baltec SCD 050 sputter

coater (Pfäffikon, Switzerland) for 40 seconds, under vacuum, at 60 mA. Furthermore, for the observation of the pyrolysed sample's surfaces, a FE-SEM Tescan S9000G (Brno, Czech Republic) was employed, using secondary electrons, 15 kV accelerating voltage, and ultrahigh-resolution conditions. ImageJ software was used to evaluate the fibre's diameters.

2.4 Processing

A self-made electrospinning apparatus was used to process all the solutions. The deposition was carried out at room temperature and relative humidity comprised between 30% and 45%. A working distance of 15 cm, 30 kV field strength, and 1.2 mL/hour flow were set to spin the βCD-based polymers, while a working distance of 15 cm, 20 kV field strength, and 0.3 mL/hour were set to process the blends of βCD-based polymer/PEO. A Linari NanoTech Easy Drum (Pisa, Italy) rotary system equipped with an aluminium cylinder was used as the collector, with a rotation speed of 75 rpm; a gauge 18 nozzle was employed.

2.5 Curing and pyrolysis

A Lenton 1200 tubular furnace was used to carry out both the curing and pyrolysis treatments. In the first case, the samples were kept at 180°C for 30 minutes, under 100 Nl/h nitrogen flow, while in the second case they were heated from room temperature to 700°C, under nitrogen flow of 100 Nl/h, with a heating rate of 10°C/ min. In both cases, the samples were maintained under nitrogen flow until room temperature was restored, after the thermal treatment.

2.6 Solubility test

For each sample, 50 mg of polymer mat were placed in a 5 mL Eppendorf tube, and then 5 mL of deionized water were added. After 24 hours at room temperature, the solution was separated from the mat via centrifugation, and the latter was dried in an oven at 60°C up to constant weight. The test was carried out in triplicate. The soluble fraction was calculated as follows,

$$Soluble\ fraction\ (\%) = \left(\frac{SMP_{before} - SMP_{after}}{SMP_{before}}\right) * 100 \quad (1)$$

where SMP_{before} and SMP_{after} represent the weights of the mat (mg) before and after the test, respectively.

2.7 Potentiometric titration

The content of free carboxylic groups present within the polymer products was determined via potentiometric titration, according to the procedure described by Soto et al., with slight modifications [98]. A 0.10M NaOH solution was used as a titrant, pre-standardized with a 25 mM oxalic acid solution. The titration was carried out by adding 0.1 mL of the titrant each step, using a volumetric burette, into the sample solution which was kept under gentle stirring and at room temperature. Titrant additions were performed at 60 seconds intervals, to allow equilibrium to be achieved. Besides, pH values were continuously measured and recorded, using a pH meter, after each addition, until the pH of 12 was reached. Subsequently, the titration curve of pH versus titrant volume was generated and the curve's inflection point was found via the second derivative approach. The volume of NaOH consumed at the inflection point was applied to the following equation, to calculate the milliequivalents of acidity per 100 g of sample:

$$\frac{m_{eq}\ of\ acidity}{100\ g\ sample} = \frac{(V_s - V_b) * C_{NaOH} * 100}{m_s} \quad (2)$$

where m_{eq} are milliequivalents, V_s and V_b are the volumes of NaOH consumed by the sample and the blank (β-CD was considered as a blank), whereas C_{NaOH} is the concentration of NaOH in mol/L, and m_s is the mass of the sample. The potentiometric titrations were performed in duplicate.

2.8 Probe molecules adsorption tests and HPLC-UV/Vis detection

Batch adsorption tests were performed starting from 25 mL of 1 and 10 mg/L atenolol water solutions, at room temperature. Calibration curves were constructed before the sample analysis, from 0.2 to 1 mg/L for the test performed at 1 mg/L and from 1 to 10 mg/L for the tests carried out at 10 mg/L. The adsorption tests were performed in triplicate by adding, in separate tests, 25 mg of the cross-linked mat or of the carbon fibres to probe solutions. All the dispersions were continuously stirred at room temperature with an orbital shaker. At fixed intervals, the concentration of atenolol was measured via HPLC-UV/Vis technique, by using a Dionex (Sunnyvale, CS, USA) consisting of a P680 pump coupled with a UVD170U detector. Separation was achieved on a Kinetex® C18 (150 x 4,6 mm, 5μm). The mobile phase consisted of 0.1% orthophosphoric acid in water and acetonitrile in the ratio of 90:10 v/v. The mobile phase was filtered through a 0.45μm nylon filter and degassed prior to use. The quantification of atenolol was performed at 230 nm while the run time for the assay was 6.5 minutes at 1mL/min. The retention time for atenolol was 4.7 min.

3. Results and discussion

3.1 Polymer characterisation

The first step of the work was focused on synthesizing a βCD-based polymer, exploiting a CHO/CIT-based NADES as a solvent, and at the same time, as a reactive media system. This was possible thanks to the capability of (i) CIT to act as the cross-linker and (ii) CHO as the functional molecule, as recently described by our group [69]. The reported mechanism involves the formation of anhydride intermediates (Figure 1A), which can easily be attacked by the hydroxyl groups of either βCD or CHO, causing the formation of ester bonds. The formation of a bridge between βCD determines the growth of the polymer chain, while a bridge between βCD and CHO forms a positively charged pendant, as reported in Figure 1B.

The presence of a product after the purification step carried out via ultrafiltration technique with a 10k Da cut-off membrane, demonstrated the occurrence of the polymerization reaction. The obtained polymer, approximately 25 wt. % of the non-purified one was subsequently characterised to also assess the presence of positively charged pendants imparted by CHO molecules. FTIR-ATR and elemental analysis measurements were performed for this purpose. Figure 2A reports the FTIR-ATR spectra of the polymer product. The peak centred at 1720 cm^{-1} and the shoulder at 1178 cm^{-1}, supported the mechanism behind the formation of ester bridges and the presence of free carboxyl functions, imparted by CIT molecules. In addition, the presence of a peak centred at approximately 1478 cm^{-1}, typical of quaternary ammonium functions, represents a starting proof of the presence of grafted ammonium groups (see the spectrum of CHO in Figure 2E). The elemental analysis of the polymer product gave a nitrogen content of 2.28±0.10 wt. %, as a confirmation of the reactions involving CHO molecules.

3.2 Electrospinning

The possibility to produce fibres and mats, with high surface-to-volume ratio and controllable structures and morphologies, is a unique feature offered by the electrospinning technique. Nevertheless, an optimization of the processing parameters is required to get fibres without defects. The parameter that most influences the process is the concentration of the polymer solution and, therefore, its viscosity, reflecting the entanglements generated between the polymer chains and proportional to the molecular weight of the latter. Consequently, the work was firstly focused on screening the optimal polymer concentration, necessary to obtain a good deposition, lack of defects on the obtained fibrous mats, and absence of difficulties such as clogging of the nozzle, during the processing step. Different amounts of polymer powder were solubilized in deionized water at room temperature, with the purpose to obtain distinct solutions with concentrations ranging from 50 wt. % to 70 wt. %, at increasing amounts of approximately 2 wt. % one to the next. After complete solubilization, the electro-spinnability of each solution was evaluated.

Figure 3 shows the results of the screening. At a concentration of 62.50 wt. % (Figure 3A, 3B) the presence of beads and short split fibres, was proof that the polymer concentration was still low. On the contrary, the clogging of the nozzle and the low deposition yield were observed while spinning the solutions at 66.67 wt. % (Figure 3G, 3H), and suggested that in that case, the concentration exceeded the optimum condition. Eventually, the best processing and produced mats were observed from polymer solutions at 64.52 wt. % (Figure 3D, 3E). In this case, the absence of beads and well-defined fibres with a mean diameter of 0.79±0.19 µm were observed as the product. Besides, at increasing polymer concentrations, an increase in the mean diameters was observed accordingly (by comparing Figure 3C, 3F, and 3I), also associated with more polydisperse systems.

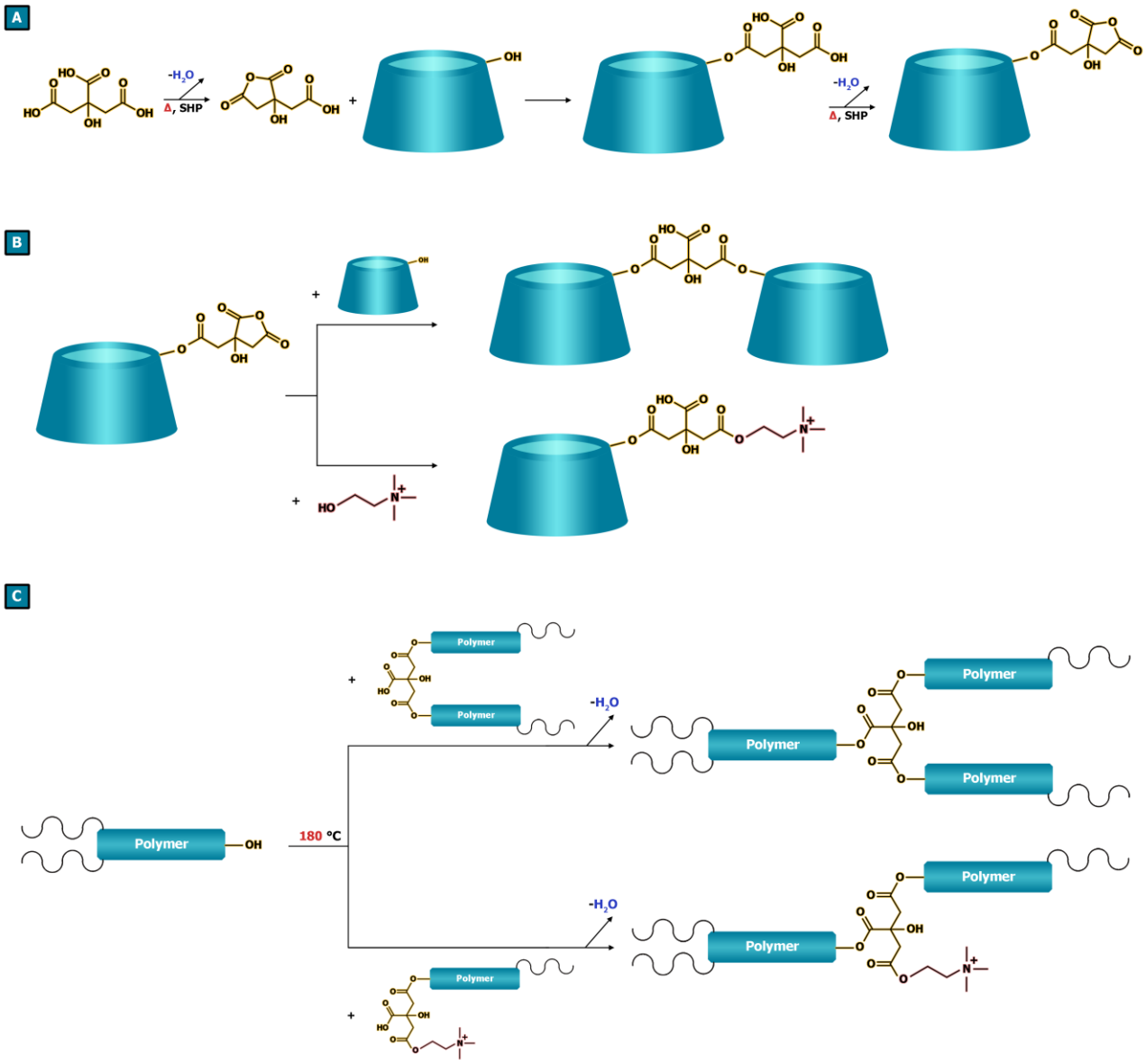

Figure 1 Reactions occurring during the synthesis of the polymer: (A) Formation of anhydride intermediates, (B) anhydride ring-opening reactions giving bridges between βCDs and bridges between βCD and CHO molecules. (C) Reactions occurring during the curing process.

3.3 Fibre's curing

After demonstrating the possibility to obtain fibrous mats from the electrospinning of the βCD-based polymer water solutions, the capability to cross-link their structure without altering the fibrous morphology, thus obtaining insoluble products, was evaluated. The fibres obtained from solutions at 64.52 wt. % were chosen to perform this study. At first, the polymer was analysed via TGA to study its thermal stability. Figure 2F (solid) shows that the fibres resulted thermally stable up to approximately 130°C, while the degradation took place in a three-step process occurring roughly between 150°C and 400°C, giving a stable carbon residue at 700°C, corresponding approximately to 18% of the initial weight. However, the weight loss phenomenon centred approximately at 180°C, evidenced by the derivative curve (Figure 2G, solid), has been attributed to the loss of water, as a product of the esterification reactions, causing the curing of the polymer structure, as reported in Figure 1C [69]. For this reason, 180°C was chosen as the temperature to perform the cross-linking process. Consequently, the weight loss associated with the esterification reactions was no longer evident after the thermal treatment (Figure 2G, dashed), confirming the hypothesized mechanism. Potentiometric titrations were exploited to quantify the number of free carboxylic groups present in the polymer before and after the thermal treatment, as further evidence of the occurrence of the esterification reactions resulting in cross-linking of the polymer. The results are expressed as milliequivalents of acidity per 100 g of the tested sample, calculated according to Eqn. 2, thus proportional to the number of carboxylic groups displayed by each sample. As a

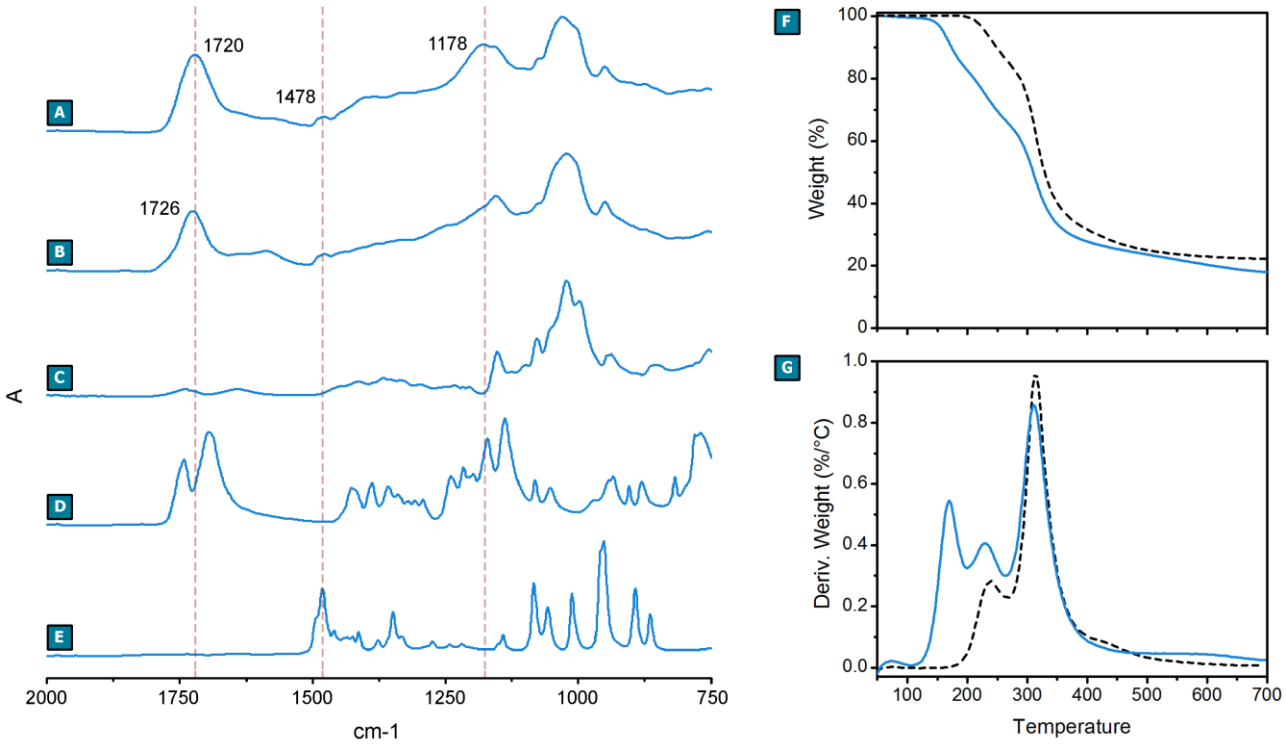

Figure 2 FTIR-ATR spectrum of water-soluble polymer (A) cured polymer (B), βCD (C), CIT (D), and (E) CHO. Water soluble polymer (solid) and cured polymer (dashed) TGA (F) and (G) DTGA curves.

result, the polymer before the thermal treatment displayed 462±3 m_{eq} of acidity, whereas the polymer after thermal treatment was characterized by 124±2 m_{eq} of acidity. The results obtained are consistent with the hypothesized mechanism (Figure 1), since the esterification reactions taking place during the curing of the mat are associated with a decrease in the number of free carboxyl groups. Eventually, after curing, the polymer resulted stable up to 200°C, while a carbon residue, corresponding approximately to 22% of the initial weight, was observed as the result of a two-step degradation process.

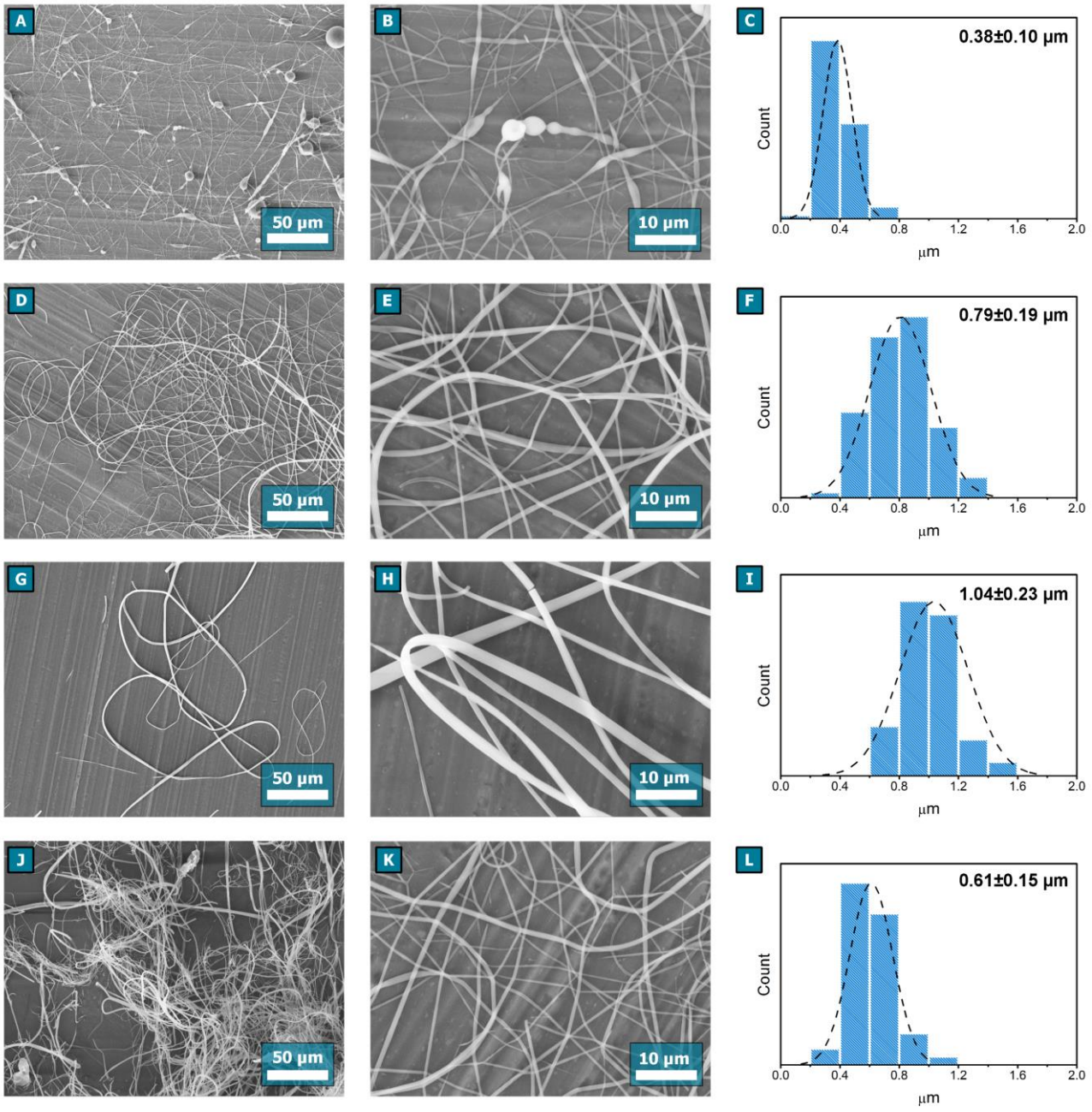

Figure 3 SEM images and diameters distributions of spun polymer fibres obtained from (A, B, and C) 62.50 wt. %, (D, E, and F) from 64.52 wt. %, and (G, H, and I) from 66.67 wt. % water solutions. (J, K, L) SEM images and diameters distributions of fibres obtained from 64.52 wt. % polymer solution, after thermal treatment at 180°C.

The morphology of the cured samples was investigated, and the results obtained (Figure 3J, 3K) clearly showed distinct fibrous mats, confirming the retention of the morphology obtained via electrospinning, after the thermal treatment. Because of the curing, a slight decrease in the fibre's diameters was detected, being the latter characterised by an average value of 0.61±0.15 μm. Eventually, water solubility tests were carried out as a further evaluation of the studied thermal curing. The mats were dipped in deionized water at room temperature and recovered via centrifugation after 24 hours. After being dried up to constant weight, the soluble fraction was calculated according to Eqn. 1 and resulted in equal to 21.6±1.1%. Hence, approximately the 80 wt. % of the starting material was recovered. This result further confirmed the occurrence of cross-linking reactions, giving a water-insoluble polymer structure, while the observed polymer loss was related to the presence of polymer chains that did not undergo a complete cross-linking, and to hydrolytic mechanisms taking place during the test. Also, the cross-linked polymer displayed a higher nitrogen content (2.92±0.01 wt. %) than the water-soluble one, caused by the water released as a condensation product. In addition, by analysing the polymer via ζ-potential analysis, a positive value of 13.1±1.3 mV was observed, imparted by the quaternary ammonium pendants related to bound CHO molecules. This feature allows the polymer to display electrostatic interactions towards negatively charged target molecules for e.g. adsorption or release applications.

3.4 Fibre's pyrolysis

In light of the significant amount of carbon residue observed as the product of the polymer thermal degradation, the electrospun βCD-based polymer mats were studied as a novel precursor to obtaining carbon fibres. Again, the fibres obtained from solutions at 64.52 wt. % were chosen for this purpose. The pyrolysis of the polymer mat was performed either (i) at ambient pressure under a 100 Nl/h nitrogen flow, or (ii) at 1 mbar pressure, via a vacuum line coupled to a rotary vane pump. In both cases, 700°C was chosen as the temperature to produce the carbon product. After the thermal treatments, the samples were studied via SEM and FE-SEM, to characterise their morphology and surface features, respectively. As reported in Figure 4, both approaches used led to samples displaying fibrous morphology, characterised by similar mean diameters of 0.49±0.10 μm in the case of nitrogen atmosphere, and 0.46±0.14 μm in the case of vacuum conditions. However, the FE-SEM images (Figure 4C, 4G) showed that the samples appeared to be characterised by slightly different surface features. In the first case (nitrogen flow, Figure 4C), an uneven surface characterised by roughness comprised between a few nanometres to 50 nm, was detected. On the other hand, in the second case (vacuum, Figure 4G), the sample appeared to be characterised by flat surfaces, where the presence of porosity was not observed. However, considering that the 80% weight loss observed because of the thermal degradation (Figure 2F) is associated to only a 20% decrease of the fibre's diameters after the pyrolysis process (Figure 3J, 3K, 3L), an overall hollow porous structure characterizing the carbon product, can be hypothesized.

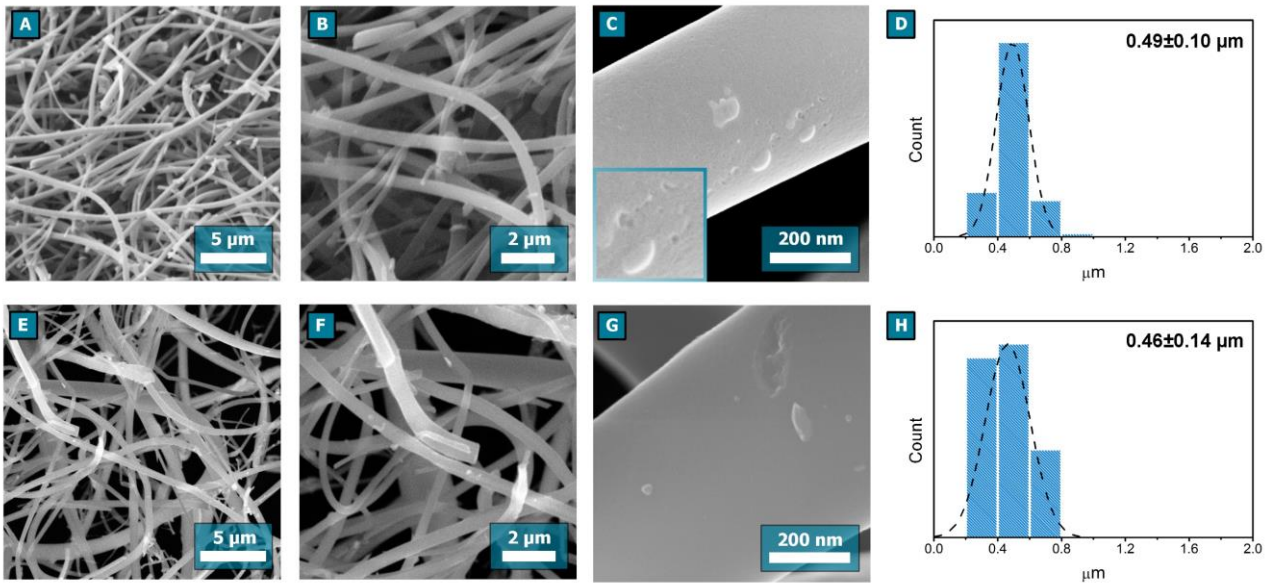

Figure 4 SEM, FE-SEM, and diameter distributions images of carbons obtained from the pyrolysis of fibrous mats, spun from a 64.50 wt. % βCD-based polymer. Thermal treatment carried out under nitrogen flow (A, B, C, D), and thermal treatment carried out under vacuum (E, F, G, H).

3.5 Porous carbons

Once assessed the capability of the reported spun mats to be exploited as suitable substrates to produce carbon sub-micrometric fibres, the last step of the work was focused on validating the possibility to tune their porosities, observed as the result of the thermal treatment. One popular approach to preparing porous carbons is to blend non-char polymers with char-forming ones, exploiting the former as pore initiation agents during the pyrolysis step. To this end, PEO has often been reported as a suitable choice [99–101]. Hence, solutions of polymer blends composed of the reported βCD-based polymer and PEO were prepared and subsequently

Blend	wt. %		Fibre's diameters (µm)	Carbon pore diameters (nm)
	βCD-based polymer	PEO		
1	0.06	0.06	0.58±0.07	\
2	0.09	0.06	0.61±0.12	\
3	0.12	0.06	1.02±0.30	\
4	0.24	0.06	1.43±0.91	24±8
5	0.36	0.06	1.87±0.26	15±6
6	0.48	0.06	1.81±0.63	13±4

Table 1. βCD-based polymer/PEO blends processed via electrospinning, resulting fibre's diameters, and carbon pore size distribution.

electrospun. Firstly, the electrospinning parameters were optimized to get fibres from PEO water solutions. Further, the deposition of well-defined fibres characterised by mean diameters of 0.46±0.07 µm was observed

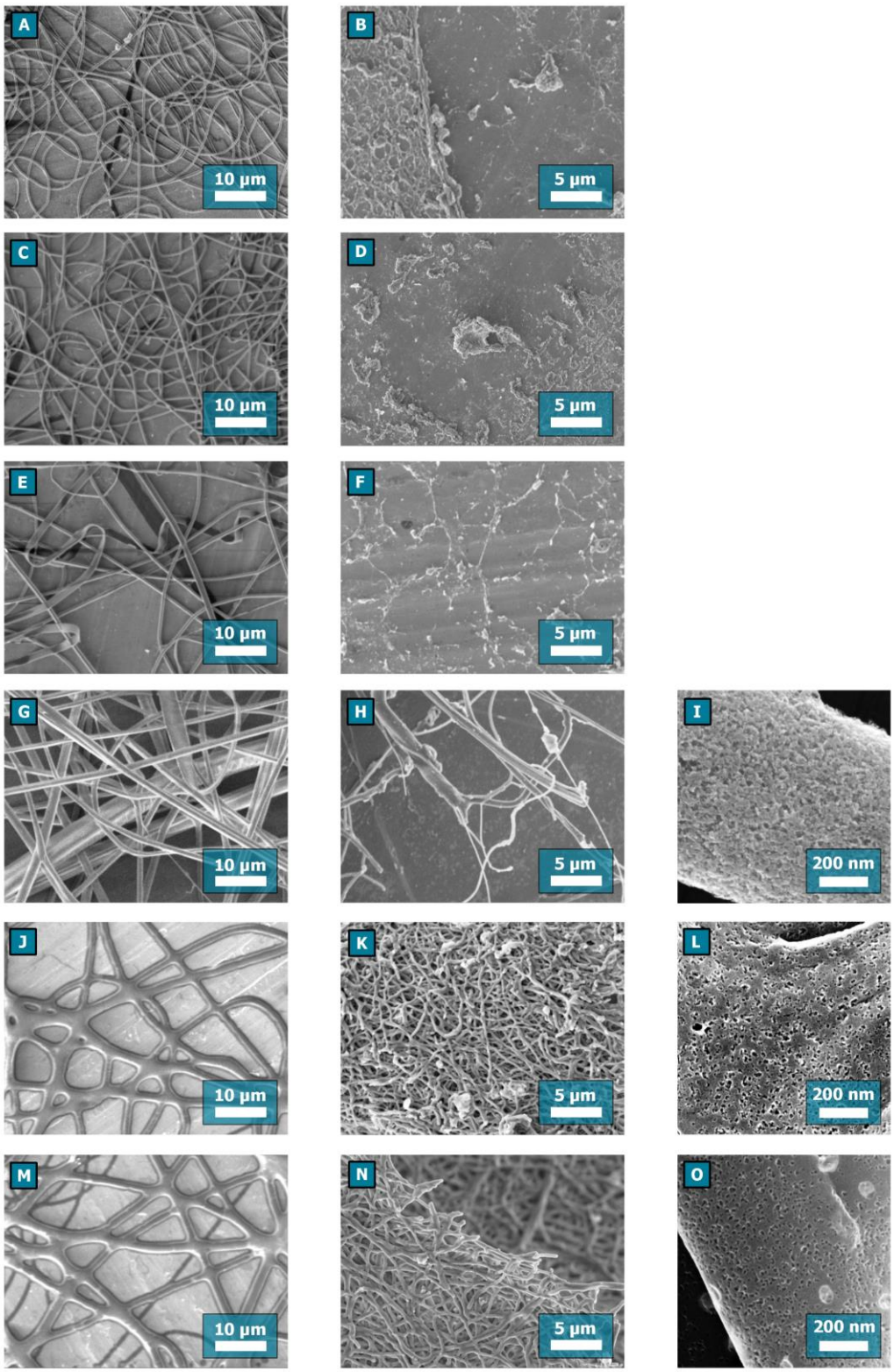

Figure 5 SEM images of spun mats (first column), resulting carbons (second column), and FE-SEM of carbon porosity (third column) obtained from: Blend 1 (A, B), Blend 2 (C, D), Blend 3 (E, F), Blend 4 (G, H, I), Blend 5 (J, K, L), Blend 6 (M, N, O).

from 5.66 wt. % solutions. Afterwards, the electro-spinnability of the different βCD-based polymer/PEO blends was tested (Table 1). As shown in Figure 5, the deposition of fibres was observed from the processing of all the blends studied. Moreover, an increase in the average fibre diameters was detected, proportional to the increasing amount of βCD-based polymer in the blend. After the electrospinning, all the mats were pyrolyzed under nitrogen flow, as previously described, and the resulting carbon products were further characterised to assess the retention of the fibrous morphology and the presence of any porosity. The pyrolysis of the mats obtained from Blend 1 and Blend 2 did not lead to fibrous products, probably due to the lower amount of βCD-based polymer compared to that of PEO. In these cases, the amount of char-forming polymer resulted too low to allow the fibrous morphology to be retained during the volatilization of PEO. Further, the presence of small fibrous domains is apparent in Figure 5F (Blend 3), suggesting that the increasing amount of βCD-based polymer might result beneficial to obtain fibrous products. As proof, from Blend 4, Blend 5, and Blend 6, fibrous carbons were obtained as pyrolysis products. The carbon fibres obtained from Blend 4 were characterised by a mean diameter of 1.23±0.56 μm, with a diameter decrease of approximately 15%, if compared to the spun mat. A decrease of the diameters of approximately 55% was observed instead from Blend 5 and Blend 6, at increasing βCD-based polymer amount, being the carbon fibres characterised by a mean diameter of 0.63±0.15 μm and 0.76±0.18 μm, respectively. This behaviour was related to the electrospinning process; as reported in Figure 5J and Figure 5M, the fibres obtained were not well-defined, but coalescence phenomena took place once they reached the collector. This feature is commonly related to a deposition carried out in a non-optimal condition, in which a fraction of solvent (distilled water), is still present in the fibres when they reach the collector (in optimal conditions, the solvent evaporates completely before the fibres reach the collector). For this reason, the fibres appear stick one to each other, characterised by larger diameters, and displaying a higher diameter decrease during the pyrolysis. Nevertheless, after a fine evaluation of the so-obtained carbon products, the presence of porosity was detected on the surfaces of the studied carbon fibres, suggesting how the solvent residues observed during the deposition did not alter the pore formation. From the pyrolysis of Blend 4 fibres, pores with an average diameter of 24±8 nm were detected, while from Blend 5 and Blend 6, pores with diameters of 15±6 nm and 13±4 nm were observed, respectively. Eventually, from the evaluation of the pores distribution, their quantities and dimensions resulted proportional to the ratio βCD-based polymer/PEO, as a confirmation of the pore-generating mechanism, the lower the amount of pore initiation agent the lower the resulting porosity.

3.5 Evaluation of adsorption performances

The cross-linked mat and the carbon fibres obtained without employing PEO, were further screened as suitable adsorbents for the removal of pollutants from contaminated water. The test was carried out by simulating water samples containing pharmaceutical products, considered emerging pollutants [102,103]. Consequently, atenolol, a beta-blocker medication used mainly to treat cardiovascular diseases, was chosen as the probe molecule [104]. The tests were carried out from 25 mL of a 10 mg/L (Figure 6A) and a 1 mg/L (Figure 6B)

atenolol distilled water solutions which were placed in contact with 25 mg of adsorbent. Subsequently, the concentration of atenolol was monitored at fixed time intervals. As a result, the crosslinked mat displayed higher adsorption performances (60.2±0.3 % from 10 mg/L, and 66.5±0.7 % from 1 mg/L) if compared to the carbon fibers (17.1±1.7 % from 10 mg/L, and 42.4±2.6 % from 1 mg/L). Further, the cross-linked mat showed a fast kinetics, reaching a plateau after approximately 30 minutes of contact between the adsorbent and the solution. Thereby, the adsorption performances observed can be related to the capability of the cross-linked mat to form stronger electrostatic interaction with the molecules of atenolol, compared to the carbon fibres, and to the possibility to generate host-guest complexes by exploiting the presence of the cavities of βCD composing the polymer chains [105].

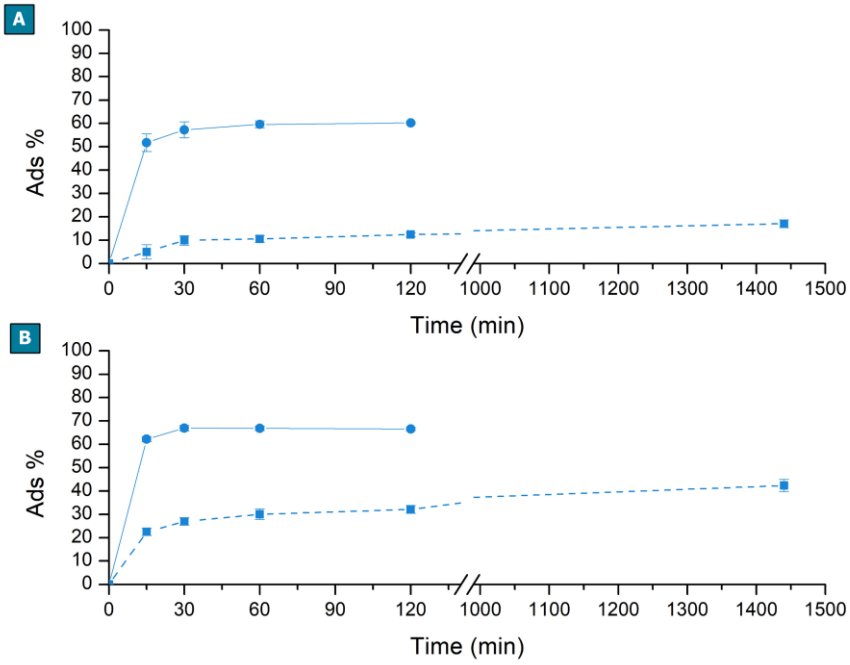

Figure 6 Atenolol adsorption tests. Adsorption profiles of cross-linked mat (solid), carbon fibres (dashed). (A) Test performed from 10 mg/L atenolol solution, and (B) test performed from 1 mg/L atenolol solution.

4. Conclusions

Citric acid/choline chloride NADES-derived beta cyclodextrin (βCD)-based polymers demonstrated to be suitable materials to obtain the deposition of bio-based fibres via electrospinning, without the use of any synthetic carrier polymer. Moreover, as a result of the intrinsic water solubility of the chosen polymers, the process was carried out using water as the unique solvent, thus exploiting a sustainable approach. An optimum condition to obtain the deposition of well-defined fibres, with diameters of 0.79±0.19 µm, was identified using 64.52 wt. % polymer solution. Subsequently, to overcome the intrinsic solubility of the obtained mats, the fibres were thermally treated via a one-step process, exploiting the presence of a residual reactivity characterizing the polymer. Thermal curing carried out at 180°C was demonstrated (i) to trigger condensation

reactions between the polymer chains, giving cross-linked, water-insoluble networks, and (ii) to retain the initial fibrous morphology, obtaining water-insoluble sub-micrometric fibres. In addition, the mats were screened as a bio-derived precursor to produce fibrous carbon materials. The pyrolysis of the spun products at 700°C, in both nitrogen flow and vacuum conditions, led to carbon materials that displayed fibrous features and fibre diameters lower than 500 nm. Furthermore, the introduction of a pore initiation agent was evaluated as an approach to tune the porosity of the previously described fibrous carbons. Different blends of βCD-based polymer and polyethylene oxide (PEO) were prepared and subsequently spun into fibres. The ratio between βCD-based polymer and (PEO) resulted to be a key factor to get the retention of the morphology after the pyrolysis, and the generation of pores. Porous carbon fibres, with pore size distribution proportional to the amount of PEO content and comprised between 13 nm and 24 nm, were obtained. Eventually, encouraging results were obtained by applying both the cross-linked mats and the carbon fibres as suitable adsorbents for the removal of pharmaceuticals, as emerging pollutants, in polluted waters. The synthesis, processing, curing, and thermal treatment chosen for this work constitute an overall sustainable process, suitable to obtain bio-based cross-linked sub-micrometric fibrous mats and carbons, which can be further studied for environmental, catalytic, pharmaceutical, and medical applications.

Author contributions

Claudio Cecone: conceptualization, methodology, investigation, validation, formal analysis, visualization, writing - original draft, writing - review & editing. Gjylije Hoti: methodology, investigation, validation, writing - review & editing. Fabrizio Caldera: supervision, methodology, writing - review & editing. Marco Zanetti: supervision, methodology, writing - review & editing. Francesco Trotta: supervision, project administration, writing - review & editing. Pierangiola Bracco: supervision, methodology, project administration, writing - review & editing.

Declaration of competing interests

The authors declare that they have no known competing financial interests or personal relationships that could have appeared to influence the work reported in this paper.

References

[1] S. Walker, R. Rothman, Life cycle assessment of bio-based and fossil-based plastic : A review, J. Clean. Prod. 261 (2020) 121158. https://doi.org/10.1016/j.jclepro.2020.121158.

[2] H. Karan, C. Funk, M. Grabert, M. Oey, B. Hankamer, Green Bioplastics as Part of a Circular Bioeconomy, Trends Plant Sci. 24 (2019) 237–249. https://doi.org/10.1016/j.tplants.2018.11.010.

[3] M.C. Bubalo, S. Vidovic, I. Radojcic, S. Jokic, Green solvents for green technologies, J Chem Technol

Biotechnol. 90 (2015) 1631–1639. https://doi.org/10.1002/jctb.4668.
[4] P.T. Anastas, J.B. Zimmerman, Design through the 12 principles of green engineering, IEEE Eng. Manag. Rev. 35 (2007) 16. https://doi.org/10.1109/EMR.2007.4296421.
[5] P.T. Anastas, N. Eghbali, Green chemistry: Principles and practice, Chem. Soc. Rev. 39 (2010) 301–312. https://doi.org/10.1039/b918763b.
[6] P.T. Anastas, M.M. Kirchhoff, Origins , Current Status , and Future Challenges of Green, Acc. Chem. Res. 35 (2002) 686–694. https://doi.org/10.1021/ar010065m.
[7] E.M. Golet, I. Xifra, H. Siegrist, A.C. Alder, W. Giger, Environmental exposure assessment of fluoroquinolone antibacterial agents from sewage to soil, Environ. Sci. Technol. 37 (2003) 3243–3249. https://doi.org/10.1021/es0264448.
[8] R. Loos, R. Carvalho, D.C. António, S. Comero, G. Locoro, S. Tavazzi, B. Paracchini, M. Ghiani, T. Lettieri, L. Blaha, B. Jarosova, S. Voorspoels, K. Servaes, P. Haglund, J. Fick, R.H. Lindberg, D. Schwesig, B.M. Gawlik, EU-wide monitoring survey on emerging polar organic contaminants in wastewater treatment plant effluents, Water Res. 47 (2013) 6475–6487. https://doi.org/10.1016/j.watres.2013.08.024.
[9] G. Bishop, D. Styles, P.N.L. Lens, Environmental performance comparison of bioplastics and petrochemical plastics : A review of life cycle assessment (LCA) methodological decisions, Resour. Conserv. Recycl. 168 (2021) 105451. https://doi.org/10.1016/j.resconrec.2021.105451.
[10] Y. Dai, J. Van Spronsen, G. Witkamp, R. Verpoorte, Y.H. Choi, Analytica Chimica Acta Natural deep eutectic solvents as new potential media for green technology, Anal. Chim. Acta. 766 (2013) 61–68. https://doi.org/10.1016/j.aca.2012.12.019.
[11] R. Craveiro, I. Aroso, V. Flammia, T. Carvalho, M.T. Viciosa, M. Dionísio, S. Barreiros, R.L. Reis, A.R.C. Duarte, A. Paiva, Properties and thermal behavior of natural deep eutectic solvents, J. Mol. Liq. 215 (2016) 534–540. https://doi.org/10.1016/j.molliq.2016.01.038.
[12] E. Durand, J. Lecomte, P. Villeneuve, From green chemistry to nature: The versatile role of low transition temperature mixtures, Biochimie. 120 (2016) 119–123. https://doi.org/10.1016/j.biochi.2015.09.019.
[13] Q. Zhang, K. De Oliveira Vigier, S. Royer, F. Jerome, Deep eutectic solvents : syntheses , properties and applications, Chem Soc Rev. 41 (2012) 7108–7146. https://doi.org/10.1039/c2cs35178a.
[14] E.L. Smith, A.P. Abbott, K.S. Ryder, Deep Eutectic Solvents (DESs) and Their Applications, Chem. Rev. 114 (2014) 11060–11082. https://doi.org/10.1021/cr300162p.
[15] A.P. Abbott, G. Capper, D.L. Davies, R.K. Rasheed, V. Tambyrajah, Novel solvent properties of choline chloride/urea mixtures, Chem. Commun. 9 (2003) 70–71. https://doi.org/10.1039/b210714g.
[16] A. Paiva, R. Craveiro, I. Aroso, M. Martins, R.L. Reis, A.R.C. Duarte, Natural Deep Eutectic Solvents − Solvents for the 21st Century, ACS Sustain. Chem. Eng. 2 (2014) 1063–1071. https://doi.org/10.1021/sc500096j.
[17] L. Kamradt, D. Carpin, N. Waszczynskyj, R.H. Ribani, C.W.I. Haminiuk, Influence of temperature,

485 water content and type of organic acid on the formation, stability and properties of functional natural
486 deep eutectic solvents, Fluid Phase Equilib. 488 (2019) 40–47.
487 https://doi.org/10.1016/j.fluid.2019.01.025.
488 [18] D. Carriazo, M.C. Serrano, M.C. Gutiérrez, M.L. Ferrer, F. Del Monte, Deep-eutectic solvents playing
489 multiple roles in the synthesis of polymers and related materials, Chem. Soc. Rev. 41 (2012) 4996–
490 5014. https://doi.org/10.1039/c2cs15353j.
491 [19] A. Di Bartolo, G. Infurna, N.T. Dintcheva, A Review of Bioplastics and Their Adoption in the Circular
492 Economy, Polymers (Basel). 13 (2021) 1229. https://doi.org/10.3390/polym13081229.
493 [20] Y. Yu, M. Shen, Q. Song, J. Xie, Biological activities and pharmaceutical applications of
494 polysaccharide from natural resources: A review, Carbohydr. Polym. 183 (2018) 91–101.
495 https://doi.org/10.1016/j.carbpol.2017.12.009.
496 [21] X. Qi, L. Wu, T. Su, J. Zhang, W. Dong, Polysaccharide-based cationic hydrogels for dye adsorption,
497 Colloids Surfaces B Biointerfaces. 170 (2018) 364–372.
498 https://doi.org/10.1016/j.colsurfb.2018.06.036.
499 [22] A. Soroudi, I. Jakubowicz, Recycling of bioplastics, their blends and biocomposites: A review, Eur.
500 Polym. J. 49 (2013) 2839–2858. https://doi.org/10.1016/j.eurpolymj.2013.07.025.
501 [23] F. Xie, E. Pollet, P.J. Halley, L. Avérous, Starch-based nano-biocomposites, Prog. Polym. Sci. 38
502 (2013) 1590–1628. https://doi.org/10.1016/j.progpolymsci.2013.05.002.
503 [24] J. Yang, Y.C. Ching, C.H. Chuah, Applications of lignocellulosic fibers and lignin in bioplastics: A
504 review, Polymers (Basel). 11 (2019) 1–27. https://doi.org/10.3390/polym11050751.
505 [25] M. Brodin, M. Vallejos, M.T. Opedal, M.C. Area, G. Chinga-Carrasco, Lignocellulosics as sustainable
506 resources for production of bioplastics – A review, J. Clean. Prod. 162 (2017) 646–664.
507 https://doi.org/10.1016/j.jclepro.2017.05.209.
508 [26] S. Ochi, Development of high strength biodegradable composites using Manila hemp fiber and starch-
509 based biodegradable resin, Compos. Part A Appl. Sci. Manuf. 37 (2006) 1879–1883.
510 https://doi.org/10.1016/j.compositesa.2005.12.019.
511 [27] H.J. Prado, M.C. Matulewicz, Cationization of polysaccharides: A path to greener derivatives with
512 many industrial applications, Eur. Polym. J. 52 (2014) 53–75.
513 https://doi.org/10.1016/j.eurpolymj.2013.12.011.
514 [28] M.R. Kweon, F.W. Sosulski, P.R. Bhirud, Cationization of waxy and normal corn and barley starches
515 by an aqueous alcohol process, Starch/Staerke. 49 (1997) 59–66.
516 https://doi.org/10.1002/star.19970490205.
517 [29] R.S. Blackburn, Natural polysaccharides and their interactions with dye molecules: Applications in
518 effluent treatment, Environ. Sci. Technol. 38 (2004) 4905–4909. https://doi.org/10.1021/es049972n.
519 [30] A. Mignon, N. De Belie, P. Dubruel, S. Van Vlierberghe, Superabsorbent polymers: A review on the
520 characteristics and applications of synthetic, polysaccharide-based, semi-synthetic and 'smart'
521 derivatives, Eur. Polym. J. 117 (2019) 165–178. https://doi.org/10.1016/j.eurpolymj.2019.04.054.

[31] J. Desbrières, E. Guibal, Chitosan for wastewater treatment, Polym. Int. 67 (2018) 7–14. https://doi.org/10.1002/pi.5464.

[32] L. Liu, Z.Y. Gao, X.P. Su, X. Chen, L. Jiang, J.M. Yao, Adsorption removal of dyes from single and binary solutions using a cellulose-based bioadsorbent, ACS Sustain. Chem. Eng. 3 (2015) 432–442. https://doi.org/10.1021/sc500848m.

[33] A. Ali, S. Ahmed, A review on chitosan and its nanocomposites in drug delivery, Int. J. Biol. Macromol. 109 (2018) 273–286. https://doi.org/10.1016/j.ijbiomac.2017.12.078.

[34] J.M. Dang, K.W. Leong, Natural polymers for gene delivery and tissue engineering, Adv. Drug Deliv. Rev. 58 (2006) 487–499. https://doi.org/10.1016/j.addr.2006.03.001.

[35] S. Bratskaya, S. Schwarz, J. Laube, T. Liebert, T. Heinze, O. Krentz, C. Lohmann, W.M. Kulicke, Effect of poly electrolyte structural features on flocculation behavior: Cationic polysaccharides vs. Synthetic polycations, Macromol. Mater. Eng. 290 (2005) 778–785. https://doi.org/10.1002/mame.200400403.

[36] K.A. Connors, The stability of cyclodextrin complexes in solution, Chem. Rev. 97 (1997) 1325–1357. https://doi.org/10.1021/cr960371r.

[37] H.J. Schneider, F. Hacket, V. Rüdiger, H. Ikeda, NMR studies of cyclodextrins and cyclodextrin complexes, Chem. Rev. 98 (1998) 1755–1785. https://doi.org/10.1021/cr970019t.

[38] M.E. Davis, M.E. Brewster, Cyclodextrin-based pharmaceutics: Past, present and future, Nat. Rev. Drug Discov. 3 (2004) 1023–1035. https://doi.org/10.1038/nrd1576.

[39] T. Loftsson, M.E. Brewster, Pharmaceutical applications of cyclodextrins. 1. Drug solubilization and stabilization, J. Pharm. Sci. 85 (1996) 1017–1025. https://doi.org/10.1021/js950534b.

[40] A. Celebioglu, Z.I. Yildiz, T. Uyar, Electrospun crosslinked poly-cyclodextrin nanofibers: Highly efficient molecular filtration thru host-guest inclusion complexation, Sci. Rep. 7 (2017) 1–11. https://doi.org/10.1038/s41598-017-07547-4.

[41] K. Uekama, F. Hirayama, T. Irie, Cyclodextrin drug carrier systems, Chem. Rev. 98 (1998) 2045–2076. https://doi.org/10.1021/cr970025p.

[42] F. Caldera, M. Tannous, R. Cavalli, M. Zanetti, F. Trotta, Evolution of Cyclodextrin Nanosponges, Int. J. Pharm. 531 (2017) 470–479. https://doi.org/10.1016/j.ijpharm.2017.06.072.

[43] G. Wenz, Cyclodextrins as Building Blocks for Supramolecular Structures and Functional Units, Angew. Chemie Int. Ed. English. 33 (1994) 803–822. https://doi.org/10.1002/anie.199408031.

[44] A.P. Sherje, B.R. Dravyakar, D. Kadam, M. Jadhav, Cyclodextrin-based nanosponges: A critical review, Carbohydr. Polym. 173 (2017) 37–49. https://doi.org/10.1016/j.carbpol.2017.05.086.

[45] F. Trotta, Cyclodextrins in Pharmaceutics, Cosmetics, and Biomedicine: Current and Future Industrial Applications, Cyclodextrins Pharm. Cosmet. Biomed. Curr. Futur. Ind. Appl. 17 (2011) 323–342. https://doi.org/10.1002/9780470926819.ch17.

[46] G. Tejashri, B. Amrita, J. Darshana, Cyclodextrin based nanosponges for pharmaceutical use: A review, Acta Pharm. 63 (2013) 335–358. https://doi.org/10.2478/acph-2013-0021.

[47] F. Trotta, Cyclodextrin nanosponges and their applications, in: Cyclodextrins Pharm. Cosmet. Biomed. Curr. Futur. Ind. Appl., First, 2011: pp. 323–342. https://doi.org/10.1002/9780470926819.ch17.

[48] F. Trotta, M. Zanetti, R. Cavalli, Cyclodextrin-based nanosponges as drug carriers, Beilstein J. Org. Chem. 8 (2012) 2091–2099. https://doi.org/10.3762/bjoc.8.235.

[49] S. Swaminathan, R. Cavalli, F. Trotta, Cyclodextrin-based nanosponges: a versatile platform for cancer nanotherapeutics development, Wiley Interdiscip. Rev. Nanomedicine Nanobiotechnology. 8 (2016) 579–601. https://doi.org/10.1002/wnan.1384.

[50] M. Gharakhloo, S. Sadjadi, M. Rezaeetabar, F. Askari, A. Rahimi, Cyclodextrin-Based Nanosponges for Improving Solubility and Sustainable Release of Curcumin, ChemistrySelect. 5 (2020) 1734–1738. https://doi.org/10.1002/slct.201904007.

[51] J.F. Feng, M. Tan, S. Zhang, B.J. Li, Recent Advances of Porous Materials Based on Cyclodextrin, Macromol. Rapid Commun. 42 (2021) 1–17. https://doi.org/10.1002/marc.202100497.

[52] M. Shringirishi, S.K. Prajapati, A. Mahor, S. Alok, P. Yadav, A. Verma, Nanosponges: A potential nanocarrier for novel drug delivery-a review, Asian Pacific J. Trop. Dis. 4 (2014) S519–S526. https://doi.org/10.1016/S2222-1808(14)60667-8.

[53] S. V. Chilajwar, P.P. Pednekar, K.R. Jadhav, G.J.C. Gupta, V.J. Kadam, Cyclodextrin-based nanosponges: A propitious platform for enhancing drug delivery, Expert Opin. Drug Deliv. 11 (2014) 111–120. https://doi.org/10.1517/17425247.2014.865013.

[54] C.Y. Xing, S.L. Zeng, S.K. Qi, M.J. Jiang, L. Xu, L. Chen, S. Zhang, B.J. Li, Poly (vinyl alcohol)/β-cyclodextrin composite fiber with good flame retardant and super-smoke suppression properties, Polymers (Basel). 12 (2020) 1–14. https://doi.org/10.3390/polym12051078.

[55] A. Alsbaiee, B.J. Smith, L. Xiao, Y. Ling, D.E. Helbling, W.R. Dichtel, Rapid removal of organic micropollutants from water by a porous β-cyclodextrin polymer, Nature. 529 (2016) 190–194. https://doi.org/10.1038/nature16185.

[56] H.L. Jiang, J.C. Lin, W. Hai, H.W. Tan, Y.W. Luo, X.L. Xie, Y. Cao, F.A. He, A novel crosslinked β-cyclodextrin-based polymer for removing methylene blue from water with high efficiency, Colloids Surfaces A Physicochem. Eng. Asp. 560 (2019) 59–68. https://doi.org/10.1016/j.colsurfa.2018.10.004.

[57] E.Y. Ozmen, M. Yilmaz, Pretreatment of Candida rugosa lipase with soybean oil before immobilization on β-cyclodextrin-based polymer, Colloids Surfaces B Biointerfaces. 69 (2009) 58–62. https://doi.org/10.1016/j.colsurfb.2008.10.021.

[58] J. Li, H. Xiao, J. Li, Y. Zhong, Drug carrier systems based on water-soluble cationic β-cyclodextrin polymers, Int. J. Pharm. 278 (2004) 329–342. https://doi.org/10.1016/j.ijpharm.2004.03.026.

[59] E.Y. Ozmen, M. Yilmaz, Use of β-cyclodextrin and starch based polymers for sorption of Congo red from aqueous solutions, J. Hazard. Mater. 148 (2007) 303–310. https://doi.org/10.1016/j.jhazmat.2007.02.042.

[60] J.A. McCune, S. Kunz, M. Olesińska, O.A. Scherman, DESolution of CD and CB Macrocycles, Chem. - A Eur. J. 23 (2017) 8601–8604. https://doi.org/10.1002/chem.201701275.

[61] T. Moufawad, L. Moura, M. Ferreira, H. Bricout, S. Tilloy, E. Monflier, M. Costa Gomes, D. Landy, S. Fourmentin, First Evidence of Cyclodextrin Inclusion Complexes in a Deep Eutectic Solvent, ACS Sustain. Chem. Eng. 7 (2019) 6345–6351. https://doi.org/10.1021/acssuschemeng.9b00044.

[62] M.E. Di Pietro, G. Colombo Dugoni, M. Ferro, A. Mannu, F. Castiglione, M. Costa Gomes, S. Fourmentin, A. Mele, Do Cyclodextrins Encapsulate Volatiles in Deep Eutectic Systems?, ACS Sustain. Chem. Eng. 7 (2019) 17397–17405. https://doi.org/10.1021/acssuschemeng.9b04526.

[63] V. Athanasiadis, S. Grigorakis, S. Lalas, D.P. Makris, Stability effects of methyl β-cyclodextrin on Olea europaea leaf extracts in a natural deep eutectic solvent, Eur. Food Res. Technol. 244 (2018) 1783–1792. https://doi.org/10.1007/s00217-018-3090-8.

[64] C. Georgantzi, A.E. Lioliou, N. Paterakis, D.P. Makris, Combination of lactic acid-based deep eutectic solvents (DES) with β-cyclodextrin: Performance screening using ultrasound-assisted extraction of polyphenols from selected native Greek medicinal plants, Agronomy. 7 (2017) 1–12. https://doi.org/10.3390/agronomy7030054.

[65] V. Athanasiadis, S. Grigorakis, S. Lalas, D.P. Makris, Methyl β-cyclodextrin as a booster for the extraction for Olea europaea leaf polyphenols with a bio-based deep eutectic solvent, Biomass Convers. Biorefinery. 8 (2018) 345–355. https://doi.org/10.1007/s13399-017-0283-5.

[66] H.N. Rajha, S. Chacar, C. Afif, E. Vorobiev, N. Louka, R.G. Maroun, β-Cyclodextrin-Assisted Extraction of Polyphenols from Vine Shoot Cultivars, J. Agric. Food Chem. 63 (2015) 3387–3393. https://doi.org/10.1021/acs.jafc.5b00672.

[67] G.C. Dugoni, M.E. Di Pietro, M. Ferro, F. Castiglione, S. Ruellan, T. Moufawad, L. Moura, M.F. Costa Gomes, S. Fourmentin, A. Mele, Effect of Water on Deep Eutectic Solvent/β-Cyclodextrin Systems, ACS Sustain. Chem. Eng. 7 (2019) 7277–7285. https://doi.org/10.1021/acssuschemeng.9b00315.

[68] M. Ferreira, F. Jérôme, H. Bricout, S. Menuel, D. Landy, S. Fourmentin, S. Tilloy, E. Monflier, Rhodium catalyzed hydroformylation of 1-decene in low melting mixtures based on various cyclodextrins and N,N′-dimethylurea, Catal. Commun. 63 (2015) 62–65. https://doi.org/10.1016/j.catcom.2014.11.001.

[69] C. Cecone, G. Hoti, I. Krabicova, S.L. Appleton, F. Caldera, P. Bracco, M. Zanetti, F. Trotta, Sustainable synthesis of cyclodextrin-based polymers exploiting natural deep eutectic solvents, Green Chem. 22 (2020) 5806–5814. https://doi.org/10.1039/d0gc02247k.

[70] J. Anu Bhushani, C. Anandharamakrishnan, Electrospinning and electrospraying techniques: Potential food based applications, Trends Food Sci. Technol. 38 (2014) 21–33. https://doi.org/10.1016/j.tifs.2014.03.004.

[71] D. Li, Y. Xia, Electrospinning of nanofibers: Reinventing the wheel?, Adv. Mater. 16 (2004) 1151–1170. https://doi.org/10.1002/adma.200400719.

[72] A. Celebioglu, F. Topuz, T. Uyar, Water-Insoluble Hydrophilic Electrospun Fibrous Mat of Cyclodextrin-Epichlorohydrin Polymer as Highly Effective Sorbent, ACS Appl. Polym. Mater. 1 (2019) 54–62. https://doi.org/10.1021/acsapm.8b00034.

[73] N. Bhardwaj, S.C. Kundu, Electrospinning: A fascinating fiber fabrication technique, Biotechnol. Adv. 28 (2010) 325–347. https://doi.org/10.1016/j.biotechadv.2010.01.004.

[74] A. Celebioglu, F. Topuz, Z.I. Yildiz, T. Uyar, Efficient Removal of Polycyclic Aromatic Hydrocarbons and Heavy Metals from Water by Electrospun Nanofibrous Polycyclodextrin Membranes, ACS Omega. 4 (2019) 7850–7860. https://doi.org/10.1021/acsomega.9b00279.

[75] R.P. Schwarzenbach, B.I. Escher, K. Fenner, T.B. Hofstetter, C.A. Johnson, U. Von Gunten, B. Wehrli, The Challenge of Micropollutants in Aquatic Systems Published by : American Association for the Advancement of Science Linked references are available on JSTOR for this article : The Challenge of Micropollutants ally used in industrial and consumer produc, Science. 313 (2006) 1072–1077. https://science.sciencemag.org/content/313/5790/1072.

[76] P.E. Stackelberg, E.T. Furlong, M.T. Meyer, S.D. Zaugg, A.K. Henderson, D.B. Reissman, Persistence of pharmaceutical compounds and other organic wastewater contaminants in a conventional drinking-water-treatment plant, Sci. Total Environ. 329 (2004) 99–113. https://doi.org/10.1016/j.scitotenv.2004.03.015.

[77] A.J. Watkinson, E.J. Murby, D.W. Kolpin, S.D. Costanzo, The occurrence of antibiotics in an urban watershed: From wastewater to drinking water, Sci. Total Environ. 407 (2009) 2711–2723. https://doi.org/10.1016/j.scitotenv.2008.11.059.

[78] E. Gonzalez, A. Barquero, B. Muñoz-sanchez, M. Paulis, J.R. Leiza, Green electrospinning of polymer latexes: A systematic study of the effect of latex properties on fiber morphology, Nanomaterials. 11 (2021) 1–14. https://doi.org/10.3390/nano11030706.

[79] C. Popov, Nanostructured Carbon Materials, in: Funct. Prop. Nanostructured Mater., 2006: pp. 387–398. https://doi.org/10.1007/1-4020-4594-8_34.

[80] W. Gu, G. Yushin, Review of nanostructured carbon materials for electrochemical capacitor applications: Advantages and limitations of activated carbon, carbide-derived carbon, zeolite-templated carbon, carbon aerogels, carbon nanotubes, onion-like carbon, and graphene, WIREs Energy Env. (2013) 10.1002/wene.102. https://doi.org/10.1002/wene.102.

[81] F. Fu, Q. Wang, Removal of heavy metal ions from wastewaters: A review, J. Environ. Manage. 92 (2011) 407–418. https://doi.org/10.1016/j.jenvman.2010.11.011.

[82] S.X. Zhang, L. Xu, Z.H. Chen, S.T. Fan, Z.J. Qiu, Z.J. Nie, B.J. Li, S. Zhang, Hierarchical porous carbon derived from green cyclodextrin metal-organic framework and its application in microwave absorption, J. Appl. Polym. Sci. 138 (2021). https://doi.org/10.1002/app.50849.

[83] M. Ahmad, A.U. Rajapaksha, J.E. Lim, M. Zhang, N. Bolan, D. Mohan, M. Vithanage, S.S. Lee, Y.S. Ok, Biochar as a sorbent for contaminant management in soil and water: A review, Chemosphere. 99 (2014) 19–33. https://doi.org/10.1016/j.chemosphere.2013.10.071.

[84] Suhas, P.J.M. Carrott, M.M.L. Ribeiro Carrott, Lignin - from natural adsorbent to activated carbon: A review, Bioresour. Technol. 98 (2007) 2301–2312. https://doi.org/10.1016/j.biortech.2006.08.008.

[85] P. González-García, Activated carbon from lignocellulosics precursors: A review of the synthesis

methods, characterization techniques and applications, Renew. Sustain. Energy Rev. 82 (2018) 1393–1414. https://doi.org/10.1016/j.rser.2017.04.117.

[86] V.K. Gupta, Suhas, Application of low-cost adsorbents for dye removal - A review, J. Environ. Manage. 90 (2009) 2313–2342. https://doi.org/10.1016/j.jenvman.2008.11.017.

[87] A. Abdul Razzaq, Y. Yao, R. Shah, P. Qi, L. Miao, M. Chen, X. Zhao, Y. Peng, Z. Deng, High-performance lithium sulfur batteries enabled by a synergy between sulfur and carbon nanotubes, Energy Storage Mater. 16 (2019) 194–202. https://doi.org/10.1016/j.ensm.2018.05.006.

[88] S. Chen, L. Qiu, H.M. Cheng, Carbon-Based Fibers for Advanced Electrochemical Energy Storage Devices, Chem. Rev. 120 (2020) 2811–2878. https://doi.org/10.1021/acs.chemrev.9b00466.

[89] B. Zhang, F. Kang, J.M. Tarascon, J.K. Kim, Recent advances in electrospun carbon nanofibers and their application in electrochemical energy storage, Prog. Mater. Sci. 76 (2016) 319–380. https://doi.org/10.1016/j.pmatsci.2015.08.002.

[90] C. Kim, Y.J. Cho, W.Y. Yun, B.T.N. Ngoc, K.S. Yang, D.R. Chang, J.W. Lee, M. Kojima, Y.A. Kim, M. Endo, Fabrications and structural characterization of ultra-fine carbon fibres by electrospinning of polymer blends, Solid State Commun. 142 (2007) 20–23. https://doi.org/10.1016/j.ssc.2007.01.030.

[91] Z. Zhou, T. Liu, A.U. Khan, G. Liu, Block copolymer–based porous carbon fibers, Sci. Adv. 5 (2019) 1–10. https://doi.org/10.1126/sciadv.aau6852.

[92] E. Frank, L.M. Steudle, D. Ingildeev, J.M. Spörl, M.R. Buchmeiser, Carbon fibers: Precursor systems, processing, structure, and properties, Angew. Chemie - Int. Ed. 53 (2014) 5262–5298. https://doi.org/10.1002/anie.201306129.

[93] N. Yusof, A.F. Ismail, Post spinning and pyrolysis processes of polyacrylonitrile (PAN)-based carbon fiber and activated carbon fiber: A review, J. Anal. Appl. Pyrolysis. 93 (2012) 1–13. https://doi.org/10.1016/j.jaap.2011.10.001.

[94] B. Wang, Y. Wang, Effect of fiber diameter on thermal conductivity of the electrospun carbon nanofiber mats, Adv. Mater. Res. 332–334 (2011) 672–677. https://doi.org/10.4028/www.scientific.net/AMR.332-334.672.

[95] M. Zanetti, A. Anceschi, G. Magnacca, G. Spezzati, F. Caldera, G.P. Rosi, F. Trotta, Micro porous carbon spheres from cyclodextrin nanosponges, Microporous Mesoporous Mater. 235 (2016) 178–184. https://doi.org/10.1016/j.micromeso.2016.08.012.

[96] A. Anceschi, G. Magnacca, F. Trotta, M. Zanetti, Preparation and characterization of microporous carbon spheres from high amylose pea maltodextrin, RSC Adv. 7 (2017) 36117–36123. https://doi.org/10.1039/c7ra05343f.

[97] C. Cecone, M. Zanetti, A. Anceschi, F. Caldera, F. Trotta, P. Bracco, Microfibers of microporous carbon obtained from the pyrolysis of electrospun β-cyclodextrin/pyromellitic dianhydride nanosponges, Polym. Degrad. Stab. 161 (2019) 277–282. https://doi.org/10.1016/j.polymdegradstab.2019.02.001.

[98] D. Soto, J. Urdaneta, K. Pernia, Characterization of Native and Modified Starches by Potentiometric

Titration, J. Appl. Chem. 2014 (2014) 1–9. https://doi.org/10.1155/2014/162480.

[99] J. Ozaki, N. Endo, W. Ohizumi, K. Igarashi, M. Nakahara, A. Oya, S. Yoshida, T. Iizuka, Novel preparation method for the production of mesoporous carbon fiber from a polymer blend, Carbon N. Y. 35 (1997) 1031–1033. https://doi.org/10.1016/S0008-6223(97)89878-8.

[100] N. Patel, K. Okabe, A. Oya, Designing carbon materials with unique shapes using polymer blending and coating techniques, Carbon N. Y. 40 (2002) 315–320. https://doi.org/10.1016/S0008-6223(01)00101-4.

[101] Y. Peng, R. Burtovyy, Y. Yang, M.W. Urban, M.S. Kennedy, K.G. Kornev, R. Bordia, I. Luzinov, Towards scalable fabrication of ultrasmooth and porous thin carbon films, Carbon N. Y. 96 (2016) 184–195. https://doi.org/10.1016/j.carbon.2015.09.060.

[102] S. Hube, B. Wu, Mitigation of emerging pollutants and pathogens in decentralized wastewater treatment processes: A review, Sci. Total Environ. 779 (2021) 146545. https://doi.org/10.1016/j.scitotenv.2021.146545.

[103] Y. Tang, M. Yin, W. Yang, H. Li, Y. Zhong, L. Mo, Y. Liang, X. Ma, X. Sun, Emerging pollutants in water environment: Occurrence, monitoring, fate, and risk assessment, Water Environ. Res. 91 (2019) 984–991. https://doi.org/10.1002/wer.1163.

[104] S. Batra, R. Bhushan, Bioassay, determination and separation of enantiomers of atenolol by direct and indirect approaches using liquid chromatography: A review, Biomed. Chromatogr. 32 (2018) 1–21. https://doi.org/10.1002/bmc.4090.

[105] R. Ficarra, P. Ficarra, M.R. Di Bella, D. Raneri, S. Tommasini, M.L. Calabrò, A. Villari, S. Coppolino, Study of the inclusion complex of atenolol with β-cyclodextrins, J. Pharm. Biomed. Anal. 23 (2000) 231–236. https://doi.org/10.1016/S0731-7085(00)00274-0.